Pis'ma v ZhETF, vol.71, iss.5, pp.298 - 303

ELECTROOPTIC MODULATION IN THE STARK–LADDER REGIME

P.Etchegoin[1)]

The Blackett Laboratory, Imperial College of Science, Technology, and Medicine
SW7 2BZ London, United Kingdom

Submitted 8 February 2000

A direct measurement of the in-plane birefringence below the absorption edge of a GaAs/AlAs superlattice (SL) under electric fields (**E**) shows a unique type of electrooptic modulation. The SL is sandwiched between two doped AlGaAs-alloy layers which play the simultaneous role of positive (p^+) and negative (n^-) contacts, as well as clad layers to achieve optical waveguiding. The p-(SL)-n structure is chosen so that, as a function of the externally applied bias, it displays Stark–Ladder Localization and the Quantum Confined Stark Effect at low and high fields, respectively. We show that this results in an electrooptic modulation in which the built-in birefringence of the SL initially decreases and shows a crossover to a quadratic increase for larger fields.

PACS: 42.79.Hp, 71.70.-d, 78.20.Ja, 78.66.-w

Among the diverse electrooptic effects found in bulk semiconductors and microstructures, those based on the modification of the absorption by an applied electric field are most commonly considered for application in amplitude modulators. The light beam is tuned in close resonance with the direct gap absorption which is, on the other hand, modified by the presence of an externally applied electric field. Bearing in mind that moderate changes in absorption may result in drastic amplitude variations of the transmitted/reflected beam, these devices provide an effective approach to modulate the light intensity. A myriad of electrooptic devices based on this principle have been constructed, including vertical [1] and waveguided modulators [2].

Conversely, changes in the linear optical properties *in the transparency region* (below the absorption edge of the structure) upon application of an external electric field are also present. A GaAs/AlAs superlattice (SL) or multiple quantum well (MQW) grown along ($\hat{z} \equiv [001]$) has the symmetry of the D_{2d}-point group and looks isotropic for light propagating with $\mathbf{k}^{light} \parallel \hat{z}$ and polarization in the $\hat{x}([100])$-$\hat{y}([010])$ plane. The reduction in symmetry brought about by an electric field **E** along $\hat{z}$ permits birefringence, which appears as a phase shift between different polarization in the plane $\perp$ to $\hat{z}$. From the symmetry point of view, the S_4 and $2C_2'$ axes of D_{2d} are removed by the electric field $\mathbf{E} \parallel \hat{z}$ and the two σ_v planes of the group no longer belong to the same class. Hence, two different optical constants appear for polarizations along $\hat{x}' \equiv (\hat{x} + \hat{y}) \equiv [110]$ and $\hat{y}' \equiv (\hat{x} - \hat{y}) \equiv \equiv [1\bar{1}0]$, respectively. A linearly polarized beam either along $\hat{x}$ or $\hat{y}$, is transformed into elliptically polarized light upon reflection or transmission along $\hat{z}$, on account of the phase-shift difference between $\hat{x}'$- and $\hat{y}'$-polarizations. The magnitude of this phase-shift, however, depends on the product of the propagation length (which is usually $\ll 1\mu$m along $\hat{z}$) and the field-induced birefringence. Accordingly, only small changes are seen in the conventional geometry of transmission or reflection perpendicular to the surface (a vertical modulator), and sensitive techniques based on acoustooptic modulation are required to observe the in plane anisotropy produced by **E** in the polarization of the light.

[1)] e-mail: p.etchegoin@ic.ac.uk

A completely different situation takes place for light propagating along the planes (i.e., $\mathbf{k}^{light} \parallel [110]$) in a waveguided modulator. In this case, the birefringence has at least two different origins, namely: (*i*) the boundary conditions of the electric field of the light at the clad layers and, (*ii*) the intrinsic birefringence of the MQW's or SL. The former exists even if the core waveguide material is isotropic, and constitutes a classical textbook example of the difference between a *transverse electric* or *magnetic* (TE- or TM-) mode in a planar waveguide [3]. The latter, however, in an intrinsic property of the bulk waveguide material based on the anisotropy of the electronic bands brought about by the presence of well-boundaries. After Refs. [4, 5], the effect of the boundary conditions can be minimized if the sample is thick enough (as compared to the wavelength λ of the light) so that the lowest order modes closely resemble the propagation of a free plane-wave in the bulk material of the waveguide. In this case, the clad layers greatly improve the efficiency of the transmission along the planes and the coupling to the external light source through total internal reflection, but the measured optical anisotropy *is an intrinsic property of the bulk material inside the waveguide.*

The application of an external **E**-field through the doped clad layers results in a modification of the electronic bands. Consequent with this change, there is a modulation of the built-in birefringence below the gap for $\mathbf{k}^{light} \perp \hat{z}$, which depends on the modification of dipole-allowed virtual transitions from valence- to conduction-band states for different polarizations [6]. The effect of an external electric field on MQW's and SL's have been extensively studied in the literature [7, 8]. In an isolated QW the effect of $\mathbf{E} \parallel \hat{z}$ on the confined sub-bands is called the Quantum Confined Stark Effect (QCSE) [9–12]. An isolated confined state of energy E_0 in a QW of thickness d and depth V_b experiences a red-shift in energy which is quadratic in the field for $ed|\mathbf{E}| < (V_b - E_0)$ (low fields). If **E** is further increased, the red-shift is $\propto |\mathbf{E}|^{\alpha}$, with $\alpha < 2$, and for even larger fields the effect is transformed into field-induced tunneling to the continuum states above the barrier. Still, another possibility exists if instead of isolated QW's we have a SL and minibands for electrons and holes. At low fields, Stark–Ladder Localization (SLL) occurs, and the minibands split into a series of equally-spaced states separated by $meEd$ ($m = \pm 1, \pm 2...$ etc) [8] (with $E \equiv |\mathbf{E}|$). Accordingly, SLL dominates the optical properties close to the absorption edge at low fields. At larger fields, the tunneling process among wells is lessened and the QCSE of isolated excitons in each QW is recovered. SLL can be obtained at room temperature and has been observed several times with optical techniques [13, 14]. Bleuse, Bastard and Voisin [15] calculated the optical absorption of the Stark–Ladder in the envelope-function approximation and obtained for a SL the important analytic result [15]:

$$\alpha(\omega) \sim \sum_{m=-\infty}^{m=+\infty} J_m^2\left(-\Delta/2eEd\right) Y\left(\omega - (\varepsilon + meEd)\right), \qquad (1)$$

where $\Delta = \Delta_c + \Delta_v$ is the total width of the electron and heavy-hole (hh) minibands and $\varepsilon = E_g + E_h + E_e$, with E_g the band-gap of the well material and $E_{e,h}$ the confinement energies for electrons and holes, respectively. Equation (1) predicts a blue-shift of the absorption edge [15] for increasing (small) E's. *In the limit where the excitons cannot tunnel to their neighboring wells, the gap of a collection of isolated excitons is half of the total miniband width Δ above the energy of the absorption edge of the SL.* This occurs at fields of the order of $|\mathbf{E}| \sim \Delta/4ed$ [15]. Likewise, once the excitons are isolated in each well, they display the quadratic red-shift of the QCSE. In practice, the effect at low fields

is less pronounced than the expected blue-shift of $\sim \Delta/2$. However, it has been already used for the construction of a modulator which transmits light close to the gap at moderate bias [16]. The blue-shift of the absorption edge observed in Ref. [16] was smaller than the thoretical prediction, but in qualitative agreement with the predictions of Ref. [15]. The existence of SLL implies a certain degree of coherence of the wavefunctions of the excitons among neighbouring wells. This coherence can be more easily lost in samples at room temprerature (RT) and with large inhomogeneous broadening, producing the crossover from SLL to the QCSE at even lower fields than those predicted by (1). Summarizing, as the field is increased we can expect a moderate blue-shift of the absorption edge revealing the presence of SLL, followed by a crossover to an inhomogeneously-broadened collection of localized excitons characterised by an absorption edge with a quadratic red-shift as a function of $\mathbf{E}$.

We now turn to the effect of the field-dependent band-structure on the birefringence. It is well known that the dielectric response in the transparency region *close to the absorption edge of a direct gap* can be thought of as coming from a dispersionless contribution of the average (Penn) gap of high-energy transitions, plus a resonant term with the first direct gap [6]. We shall evaluate the optical response in the transparency region at energies which are only $\sim$ 10% below the gap (ω_{gap}) and, accordingly, the shift of the absorption edge with the applied $\mathbf{E}$ ought to be the leading effect in the modification of the birefringence [17]. We shall show that in our case, a blue(red)-shift of the absorption edge corresponds to a decrease (increase) in the leading resonance term with the direct gap and, thus, to a decrease (increase) in the birefringence $\Delta n(\omega)$ close to the gap (with $\omega < \omega_{gap}$).

In this paper we measure the birefringence for in-plane propagation of light ($\mathbf{k} \perp \hat{z}$) in a thick superlattice (to minimize waveguiding effects) using the method of transmission through crossed polarizers. The light source is a Ti-Shappire laser and the sample must be properly masked to avoid stray-light and accommodate, at the same time, the electrical contacts. Further details of the experimental setup and methods were given elsewhere [4, 5]. Measurements are performed on a 300 periods, GaAs/AlAs-SL (3/0.9 nm) sandwiched between n^+- and p^+-$Ga_{0.3}Al_{0.7}As$ layers doped to 1×10^{18} cm^{-3}, which shows SLL at RT [14]. This sample is entirely equivalent to the one in Ref. [14] (where SLL at RT has been reported for the first time) except for the fact that our sample has more periods to increase the thickness along $\hat{z}$. As a characterization measurement, we show in Fig.1 the RT photocurrent spectra at zero bias. Upto six Stark–Ladder levels could be observed in close resemblance with the results of Ref. [14]. These peaks spread and outline the characteristic fan-chart of SLL for small reverse biases. We shall not dwell into the details of the photocurrent-spectra, which are already explained elsewhere [14].

Fig.2 shows the raw in-plane transmission through crossed polarizers below the gap for a sample with transmission length $l = 1.9$ mm. The data were taken for $\mathbf{k}^{light} \parallel [110]$ and both, incident and output polarizations at 45° with respect to $\hat{z}$. The birefringence oscillations (fringes) in the normalized transmitted intensity are expected to be given by [4, 5]:

$$I/I_0 \sim \cos^2\left[(\pi l/\lambda)\Delta n(\omega)\right]. \tag{2}$$

Note that the extinction point, i.e. the energy at which the oscillations vanish, can be seen to red-shift for large fields with a naked eye. The blue-shift at low fields is not seen here because the extinction point is normally a poor measure of small changes

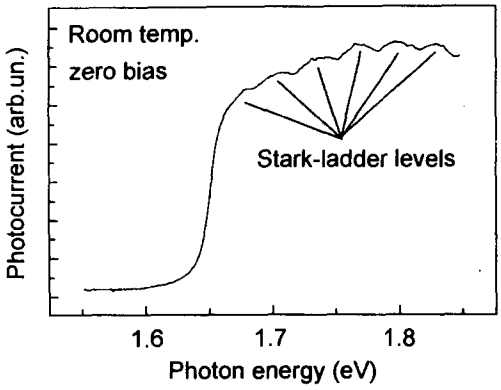

Fig.1. RT-photocurrent spectra at zero bias. See the text for further details

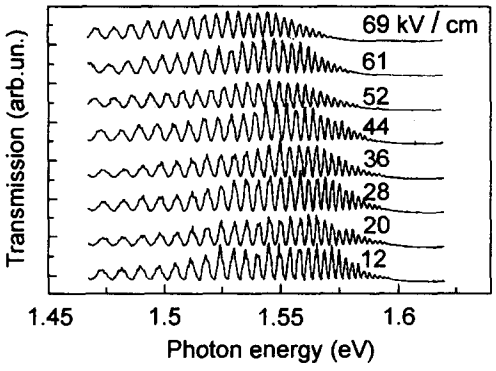

Fig.2. Raw in-plane transmission data between crossed polarizers for different applied fields. Note the red-shift of the extinction point for large fields

in the gap. The number of fringes per unit energy increases as the gap is approached from below, as expected [4, 5] from the resonant behavior of $\Delta n(\omega)$. In Fig.3 we show a blowup of the fringes in Fig.2 around $\sim$ 1.49 eV, together with their porcentual energy change. According to (2), each maximum in Fig.3a is expected to fulfill the condition $l\omega\Delta n(\omega)/2\pi c = M$, where M is a fixed large integer number. For small perturbations of the birefringence, a blue(red)-shift in the energy position of a particular fringe must be compensated by a corresponding decrease (increase) of $\Delta n(\omega)$. Since $M \gg 1$ close to the gap, differences between M and $M+1$ are negligible and successive maxima show the same porcentual energy change as shown in Fig.3b. Note also that there is a clear crossover between two distinct regions around $\sim$ 35 kV/cm. We take the energy shifts of specific fringes in Fig.3a as a clear indication of two different regimes in the electrooptic modulation of $\Delta n(\omega)$ below ω_{gap}, to wit: a blue-shift of the gap at small fields, followed by a quadratic red-shift above $\sim$ 35 KV/cm. These two regimes correspond to a decrease of the intrinsic $\Delta n(\omega)$, followed by a quadratic increase, respectively.

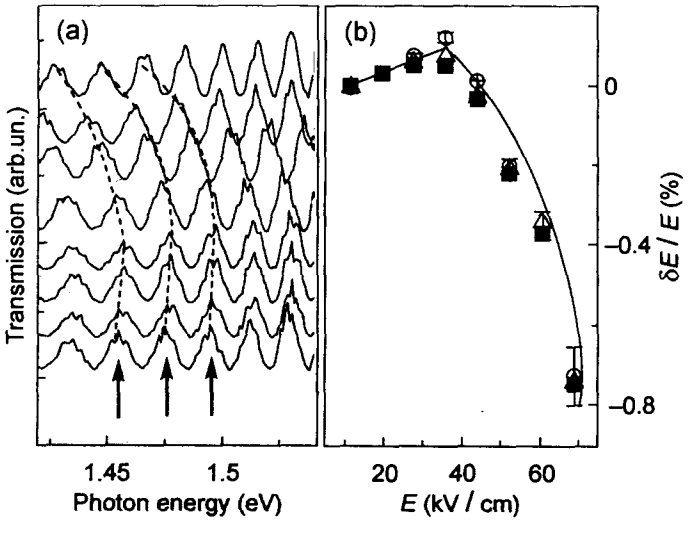

Fig.3. (a) Birefringence fringes around $\sim$ 1.49 eV which were continuously followed as a function of the extenally applied field. In (b) we show the porcentual energy change in the position of three successive fringes. Note a clear crossover between two distinct regimes around $\sim$ 35 KV/cm. See the text for further details

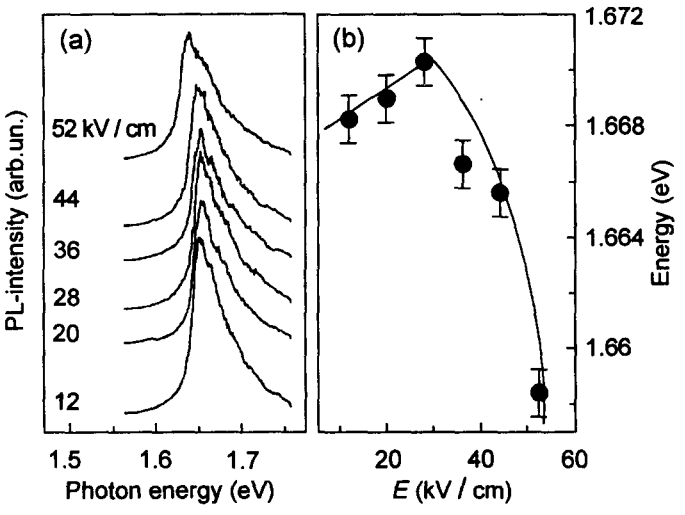

Fig.4. (a) PL data for different E's. In (b) we show the position of the average gap for different fields as obtained from the luminescence profiles. A consistent picture with the change in the birefringence fringes of Fig.3 is obtained

Very recently [17], we have shown in a systematic study of the in-plane birefringence of MQW's that a good empirical approximation for the $\Delta n(\omega)$ at energies below (but close) to the absorption edge is given by

$$\Delta n(\omega) = \Delta n^0 \frac{\omega_0}{\omega} + \frac{\hbar\Omega}{\hbar\omega} \ln\left[\frac{(\omega_g - \omega_0)\omega}{\omega_0(\omega_g - \omega)}\right], \tag{3}$$

where ω_g corresponds to the *average gap* of the SL, Δn^0 is a calibration value at $\omega_0 (< \omega_g)$, and $\hbar\Omega$ is an empirically determined parameter of the order of ~ 0.02 eV (depending on the size of the wells). For small porcentual changes, Eq. (3) can be linearized and, in this description, the field-induced changes in $\Delta n(\omega)$ should have their counterpart in the position of the average gap. A possible method for the determination of the average gap is to evaluate the mean energy (ω_g) using the luminescence profile (PL) $I(\omega)$ as a weighting factor. This determination is qualitative, for the general shape of $I(\omega)$ depends on the product of the joint density of states and the Boltzmann factor but, nevertheless, should be consistent with the overall picture. Fig.4a displays the PL-data at RT for different applied electric fields together with the average gaps calculated as $\omega_g = \int \omega I(\omega) d\omega$. The PL signals are normally faint in our experimental conditions simply because the presence of the mask for the in-plane transmission experiments implies that the data must be excited and collected from the side of the wafer, together with the fact that data are taken at RT, and that low excitation powers are used in order to leave the internal bias of the device unaltered. Notwithstanding, it is quite clear that the qualitative behaviour of ω_g in Fig.4b is in excellent agreement with the data in Fig.3b. The shift of the average gap together with the description given by Eq. (3) produces exactly the sort of modulation in the birefringence seen in Fig.3a and reveals the microscopic origin of this peculiar electrooptic effect which shows a crossover between two distinct regimes.

In conclusion, we have shown that a peculiar kind of electrooptic modulation of $\Delta n(\omega)$ in the transparency region $(\omega < \omega_{gap})$ exists in p^+-SL-n^--structures where SLL is followed by the QCSE. From the total miniband width of our sample ($\Delta \sim 10$ meV) and the period of the superlattice ($d = 4.1$ nm), the excitons should be completely localized at [15] $E \sim$ ~ 250 KV/cm. The crossover occurs, however, at fields which are about six times smaller

than the theoretical prediction of Ref. [15], which does not take into account disorder (inhomogeneous broadening) and finite temperature. The blue shift of the absorption edge at low fields is also much less than $\Delta/2$ (as observed also in Ref. [16]). The qualitative agreement with what is expected for the absorption, and its effect on $\Delta n(\omega)$ below the gap are, however, correct. Unlike the conventional Pockels- or Kerr-electrooptic modulation [3] which are monotonous with the applied field, there is in this case a crossover in both, the sign and the field-dependence of the modulation in $\Delta n(\omega)$ as a function of $\mathbf{E}$. Peculiar electrooptic applications of this effect could be envisioned.

Discussions with M. Cardona and A. Fainstein are gratefully acknowledged, P.E. wishes to thank the European Union for financial support at the Cavendish Laboratory, Cambridge, UK, where part of this work has been performed. We are indebted to D.Ritchie and M.P.Grimshaw for growing the samples.

---

1. R.Schwedler, H.Mikkelsen, K.Wolter et al., J. Phys. III France **4**, 2341 (1994).
2. E.Bigan and Ph.D.Thesis, Université de Paris-Sud (1991); S.M.Sze, *Physics of Semiconductor Devices*, Wiley, New York, 1981.
3. A.Yariv, *Optical Electronics*, Saunders HBJ, New York, 1991.
4. A.Fainstein, P.Etchegoin, P.V.Santos et al., Phys. Rev. **B50**, 11 850 (1994).
5. P.Etchegoin, A.Fainstein, A.A.Sirenko et al., Phys. Rev. **B53**, 13 662 (1996).
6. M.Cardona, in *Atomic Structure and Properties of Solids*, Ed. E.Burstein, Academic, New York, 1972, p. 513.
7. M.Jaros, *Physics and Applications of Semiconductor Microstructures*, Clarendon Press, Oxford, 1989; P.Yu and M.Cardona, *Fundamentals of Semiconductors*, Springer, Berlin, 1995; H.Haug and S.W.Koch, *Quantum Theory of the Optical and Electronic Properties of Semiconductors*, World Scientific, London, 1993.
8. E.E.Mendez, in *Optics of Semiconductor Nanostructures*, Eds. F.Henneberger, S.Schmitt-Rink, and E.O.Göbel, VCH, Weinheim, 1993.
9. E.J.Austin and M.Jaros, Phys. Rev. **B31**, 5569 (1985).
10. G.Bastard, E.E.Mendez, L.L.Chang, and L.Esaki, Phys. Rev. **B28**, 3241 (1983).
11. D.A.B.Miller, D.S.Chemla, T.C.Damen et al., Phys. Rev. **B32**, 1043 (1985).
12. D.A.B.Miller, D.S.Chemla, and S.Schmitt-Rink, Phys. Rev. **B33**, 6976 (1986).
13. E.E.Mendez and G.Bastard, Physics Today **46**(6), 34 (1993); E.E.Mendez, F.Agulló-Rueda, and J.M.Hong, Phys. Rev. Lett. **60**, 2426 (1988).
14. K.Fujiwara, Jap. J. of Appl. Phys. **28**(10), **L** 1718 (1989).
15. J.Bleuse, G.Bastard, and P.Voisin, Phys. Rev. Lett. **60**, 220 (1988).
16. E.Bigam, M.Allovon, M.Carre, and P.Voisin, Appl. Phys. Lett. **57**, 327 (1990).
17. A.A.Sirenko, P.Etchegoin, A.Fainstein et al., Phys. Rev. **B60**, 8253 (1999); Phys. Stat. Solidi (b) **215**, 241 (1999).